HHS Public Access

Author manuscript

Glia. Author manuscript; available in PMC 2023 April 01.

Published in final edited form as:

Glia. 2022 April ; 70(4): 697–711. doi:10.1002/glia.24134.

Compromised Fractalkine Signaling Delays Microglial Occupancy of Emerging Modules in the Multisensory Midbrain

Cooper A. Brett[1], **Julianne B. Carroll**[1], **Mark L. Gabriele**[1]

[1]Dept. of Biology, James Madison Univ, Harrisonburg, VA, USA

Abstract

Microglial cells (MGCs) are highly dynamic and have been implicated in shaping discrete neural maps in several unimodal systems. MGCs respond to numerous cues in their microenvironment, including the neuronally-expressed chemokine, fractalkine (CX3CL1), via interactions with its corresponding fractalkine receptor (CX3CR1). The present study examines microglial and CX3CL1 patterns with regard to the emerging modular-extramodular matrix organization within the lateral cortex of the inferior colliculus (LCIC). The LCIC is a multisensory shell region of the midbrain inferior colliculus where discrete compartments receive modality-specific connections. Somatosensory inputs terminate within modular confines, while auditory inputs target the surrounding matrix. Glutamic acid decarboxylase (GAD) is an established marker of LCIC modules in developing mouse. During early postnatal development, multimodal LCIC afferents segregate into discrete, neurochemically-defined compartments. Here, we analyzed neonatal GAD67-GFP and CX3CR1-GFP mice to assess: (1) whether MGCs are recruited to distinct LCIC compartments known to be undergoing active circuit assembly, and (2) if such behaviors are fractalkine signaling-dependent. MGCs colonize the nascent LCIC by birth and increase in density until postnatal day 12 (P12). At the peak critical period (P4-P8), MGCs conspicuously border emerging LCIC modules, prior to their subsequent invasion by P12. CX3CL1 expression becomes distinctly modular at P12, in keeping with the notion of fractalkine-mediated recruitment of microglia to modular centers. In $CX3CR1^{GFP/GFP}$ mice with compromised fractalkine signaling, microglial recruitment into modules is delayed. Taken together, these results suggest a potential role for microglia and fractalkine signaling in sculpting multisensory LCIC maps during an early critical period.

*Mail Correspondence to: Dr. Mark L. Gabriele, Ph.D., Professor, James Madison University, Department of Biology, MSC 7801, 951 Carrier Drive, Harrisonburg, Virginia 22807, phone: (540) 568-6333, gabrieml@jmu.edu.

AUTHOR CONTRIBUTIONS

CB and MG designed all experiments. CB and JC performed all experimentation. CB performed all imaging and sampling for quantification. CB and MG analyzed and interpreted the data. MG prepared all figures. MG wrote the manuscript.

CONFLICT OF INTERESTS

The authors declare that the research was conducted in the absence of any commercial or financial relationships that could be construed as a potential conflict of interest.

ETHICS APPROVAL

All experiments involving animals were performed using procedures approved by the Institutional Animal Care and Use Committee of James Madison University (approval number, 20-1421).

Keywords

microglia; fractalkine; CX3CR1; CX3CL1; multimodal; mapping; modularity; matrix; RRID: AB_839504; RRID: AB_2276839; RRID: AB_2278725; RRID: AB_2336833; RRID: AB_2336408; RRID:SCR_003070

1. INTRODUCTION

Microglia cells (MGCs) are tissue specific macrophages of the central nervous system that are yolk sac derived and colonize the embryonic brain (Ginhoux, Lim, Hoeffel, Low, & Huber, 2013; Li & Barres, 2018; Thion, Ginhoux, & Garel, 2018). Beyond their documented involvement in certain neurodegenerative disease states and in response to injury (Hong, Dissing-Olesen, & Stevens, 2016; Tay, Savage, Hui, Bisht, & Tremblay, 2017; Allen & Lyons, 2018), microglia are now known to play a prominent role in the healthy brain (Tremblay et al., 2011). MGC heterogeneity is especially diverse during early critical periods of development (Hammond et al., 2019; Masuda et al., 2019; Tan, Yuan, & Tian; 2020), as they perform a variety of functions, among them monitoring specific regions undergoing active circuit assembly. Niches of MGCs localize to areas of network construction via crosstalk with neurons and other glia in the surrounding environment and are required for selective pruning of underutilized synapses in an activity-dependent manner (Schafer & Stevens, 2015; Frost & Schafer, 2016). Such behaviors are largely transient, as MGCs trend towards a more homogenous distribution as critical periods close, exhibiting decreased engulfment activity and increasingly ramified morphologies, indicative of shifts to surveilling states (Li & Barres, 2018).

Disruption of MGC recruitment and participation in neural map remodeling are thought to contribute, in part, to certain neurodevelopmental conditions (Frick, Williams, & Pittenger, 2013; Zhan et al., 2014; Hong, Dissing-Olesen, & Stevens, 2016; Thion & Garel, 2017) including autism spectrum disorders (ASD). Several signaling mechanisms influence directed microglial migration towards emerging maps, as well as their subsequent role in the refinement process. Among them, the fractalkine signaling pathway plays a particularly critical role in regulating the sculpting of original map configurations and their functional maturation. Fractalkine (or CX3CL1), a neuronally expressed chemokine, communicates directly with microglia uniquely expressing its cognate receptor, CX3CR1 (Jung et al., 2000; Mizutani et al., 2012). With both tethered and soluble forms, fractalkine can regulate MGC recruitment/motility, as well as elimination of supernumerary synapses, although these roles appear to be somewhat system-specific. (Paolicelli et al., 2011; Paolicelli, Bisht, & Tremblay, 2014; Squarzoni et al., 2014). Deficiency or loss-of-function of fractalkine signaling impairs occupancy and functional development of barrel fields (Hoshiko, Arnoux, Avignone, Yamamoto, & Audinat, 2012; Gunner et al., 2019), as well as synaptic-dendritic spine pruning in hippocampus (Paolicelli et al., 2011; Paolicelli, Bisht, & Tremblay, 2014). CX3CR1 deficient mice exhibit decreased MGCs during early critical periods, MGC morphological changes, delayed synaptic maturation, and increased autism-related behavioral phenotypes (e.g. decreased social interaction, increased repetitive behaviors; Zhan et al., 2014).

One hallmark of MGCs in unimodal sensory structures that exhibit discrete mapping characteristics (Luo & Flanagan, 2007) is their recruitment towards, and recognition of, emerging compartmental boundaries during early development. In somatosensory cortex, microglia border emerging barrels at P5, before invading and pruning excess thalamocortical connections. Discrete CX3CL1 expression in barrel centers from P5-P10 signals MGC entry, which is delayed in mice with compromised fractalkine signaling (Hoshiko, Arnoux, Avignone, Yamamoto, & Audinat, 2012). MGCs also surround ipsi-contra borders in visual thalamus (Schafer et al., 2012), as well as glomerular borders in the olfactory system during comparable early postnatal windows (Fiske & Brunjes, 2000).

Despite the fact that impairments in certain multisensory processing tasks (e.g. multisensory binding) are highly predictive of onset and severity of symptoms associated with ASD (Collignon et al., 2013; Stevenson, Segers, Ferber, Barense, & Wallace, 2014; Stevenson et al., 2014a; Stevenson et al., 2014b; Ainsworth, Ostrolenk, Irion, & Bertone, 2021), the role that MGCs play in the functional maturation of multimodal networks remains unaddressed. Here, we begin to explore potential MGC involvement in multisensory network shaping utilizing the lateral cortex of the inferior colliculus (LCIC) as a model structure. The LCIC is a shell region of the midbrain inferior colliculus (IC) comprised of distinct compartments that receive modality-specific inputs. A series of discontinuous modular zones that span LCIC layer 2 (Chernock, Larue, &Winer, 2004) receive inputs of somatosensory origin, while the surrounding extramodular matrix is the target of converging auditory inputs (Lesicko, Hristova, Maigler, & Llano, 2016). Identified neurochemical markers (for modules: glutamic acid decarboxylase, GAD, among others; for matrix: calretinin: CR) highlight these complementary compartments that emerge in mouse during the early postnatal period (Dillingham, Gay, Behrooz, & Gabriele, 2017). Spatial and temporal alignment of discrete Eph-ephrin guidance patterns (Gabriele et al., 2011; Cramer & Gabriele, 2014; Wallace, Harris, Brubaker, Klotz, & Gabriele, 2016; Gay, Brett, Stinson, & Gabriele, 2018; Stinson, Brett, Carroll, & Gabriele, 2021) and concurrent segregation of initially intermingling multimodal projection distributions into appropriate target zones (Lamb-Echegaray, Noftz, Stinson, & Gabriele, 2019) define a critical period for the LCIC extending from birth through P12.

In the present study, we utilized immunocytochemical approaches in GAD-GFP and CX3CR1-GFP knock-in mouse lines to determine the presence/positioning of MGCs relative to emerging LCIC compartments, and whether MGC recruitment to discrete LCIC zones undergoing active circuit assembly is fractalkine signaling-dependent (Figure 1). We demonstrate that MGC density in the LCIC increases over the defined critical period and that fractalkine receptor signaling mutants exhibit diminished MGC recruitment to the LCIC, as well as delayed occupancy of its characteristic modular fields.

2. METHODS

2.1 Animals

Experiments were performed on GAD67-GFP (n = 29) and CX3CR1-GFP mice (n = 38) (JAX 00582, Jackson Laboratories) knock-in mice. The GAD67-GFP line served as controls for assessing MGC location during normal development with respect to emerging LCIC

compartments (i.e. GAD-positive modules). For details on generation of this specific strain see Tamamaki, Yanagawa, Tomioka, Miyazaki, Obata, & Kaneko, 2003 (permission granted by Dr. Yuchio Yanagawa, Gunma University Graduate School of Medicine, Gunma, Japan; breeding pairs furnished by Dr. Peter Brunjes, University of Virginia, Charlottesville, VA). This line was previously validated in our lab concerning GAD specificity in the neonatal IC (Gay, Brett, Stinson, & Gabriele, 2018). CX3CR1-GFP mice were used to visualize MGCs expressing the fractalkine receptor (microglia in both hetero- and homozygous animals express GFP), as well as to assess fractalkine signaling influences on LCIC MGC recruitment and motility ($CX3CR1^{+/GFP}$ mice retain functional signaling; $CX3CR1^{GFP/GFP}$ mice are incapable of fractalkine signaling). Both strains were bred on a C57BL/6J background (JAX 000664). Equal numbers of male and female subjects were used for each experiment (no sex-specific differences were observed). Equally spaced developmental ages were examined spanning the defined LCIC critical period (birth through P12), as well as a timepoint shortly after LCIC compartments are established and its multimodal afferent arrays are fully segregated (P16).

GAD-GFP breeding involved pairing heterozygous males with C57BL/6J females. GFP-expressing progeny were identified under a Dark Reader Spot Lamp with viewing goggles specific for GFP visualization before P4 (www.clarechemical.com, Clare Chemical Research, Cat# SL10S). Gentopying for CX3CR1-GFP mice was outsourced through Transnetyx (https://www.transnetyx.com/). Probes in the Transnetyx database specific for this JAX line were used. All experiments were performed in compliance with the US National Research Council's Guide for the Care and Use of Laboratory Animals, the US Public Health Service's Policy on Humane Care and Use of Laboratory Animals, and received prior approval from the Institutional Animal Care and Use Committee (Protocol No. 20-1421).

2.2. Tissue preparation

Mice were administered a lethal cocktail of a ketamine (200mg/kg) and xylazine (20mg/kg) before being transcardially perfused with a physiologic rinse solution (0.9% NaCl and 0.5% $NaNO_2$ in dH_2O), followed by 4% paraformaldehyde (pH 7.4), and finally a 4% paraformaldehyde with 10% sucrose solution. Brains were harvested from the skull and post-fixed overnight at 4°C in the same 4% paraformaldehyde/10% sucrose solution. Once tissue was equilibrated, it was moved to a 4% paraformaldehyde/30% sucrose for an additional night before sectioning. Brains were conservatively blocked in the coronal plane, preserving the entirety of the midbrain. Sections were taken through the caudorostral extent of the IC using a sliding freezing microtome at 50μm and collected into 0.1M phosphate buffered saline (PBS, pH 7.4).

2.3. Immunohistochemistry

Tissue sections were washed three times in PBS for 8 minutes then blocked in 5% normal horse serum (NHS). Sections were then placed in a solution with primary antibody (see Table 1; anti-Iba1, made in rabbit, 1:1000, Wako Chemicals, 019–19741, RRID: AB_839504; anti-CX3CL1/fractalkine, made in goat, 1:100, R&D Systems, AF472, RRID: AB_2276839) and incubated overnight at 4°C while being agitated. For GAD67

immunohistochemistry, a monoclonal mouse anti-GAD67 antibody (clone 1G10.2, 1:100, MilliporeSigma, MAB5406, RRID: AB_2278725) was used while employing a Species-On-Species Detection Kit (Mouse on Mouse [M.O.M.] Basic Kit, Vector Laboratories, BMK-2202, RRID: AB_2336833) in order to distinguish between endogenous mouse IgG presence and the applied primary antibody. Vector M.O.M. immunodetection protocol was performed as per vendor suggestions. Species specific biotinylated secondary antibodies were used for signal amplification and visualized with a streptavidin fluorescent conjugate (DyLight 549 streptavidin, 1:200, Vector Laboratories, SA-5549, RRID: AB_2336408).

2.4. Image acquisition

Widefield image capturing was performed on a Nikon Eclipse Ti2 microscope (Nikon, Melville, NY) equipped with a Hamamatsu ORCA-Flash4.0 V3 Digital CMOS monochrome camera for fluorescent imaging of separate channels (Hamamatsu, Bridgewater, NJ) using PlanApo 10x, 20x, and 40x objectives (NA = 0.45, 0.75, and 0.95, respectively). Filter sets (Chroma Technology, Bellows Falls, VT) were carefully selected to ensure no bleed-through between channels of the various fluorophores used (GFP filter set: excitation 446–486nm, emission 500–550; streptavidin DyLight 549 filter set: excitation 542–566, emission 582–636). Image capturing was performed using Nikon NIS-Elements Advanced Research software version 5.11.01. Separate channels imaged for each fluorophore were pseudocolored and merged. An extended depth of focus (EDF) algorithm was used to flatten 10x, 20x, and 40x Z-stacks into two-dimensional images, only showing focused regions of each optical slice. Images were taken throughout the caudorostral extent of the IC. After imaging, individual channel lookup tables (LUTs) were consistently adjusted such that sliders were positioned at the ends of the signal histogram, thereby best depicting labeling as observed through the microscope. All images were saved out of Nikon Elements as lossless JPEG2000 files.

2.5. Defining LCIC modules and sampling GAD/CX3CL1 signal periodicities

LCIC modularity was most apparent in mid-rostrocaudal sections. Raw JPEG2000 images from this region of interest were opened in NIS-Elements and exported as uncompressed TIFF files (channels of digital merges were first separated and converted to grayscale) and imported into ImageJ software (https://imagej.net/, NIH, Bethesda, MD, RRID:SCR_003070) in order to (1) aid in the objective identification of LCIC modular domains, and (2) generate brightness plot profiles for GAD/CX3CL1 sampling. GAD channels were smoothed (filter: Gaussian blur, radius = 20.0 pixels) and inverted, prior to performing a threshold function (level: 200) to aid in the objective identification of LCIC layer 2 modular fields (Figure 2). Contiguous layer 2 domains in keeping with the size/morphology of previously characterized emerging LCIC modules (Dillingham, Gay, Behrooz, & Gabriele, 2017; Gay, Brett, Stinson, & Gabriele, 2018; Lamb-Echegaray, Noftz, Stinson, & Gabriele, 2019; Stinson, Brett, Carroll, & Gabriele, 2021) were best fit with encompassing contours to define modular boundaries. GAD/CX3CL1 sampling focused on P12, as this was the initial age showing discrete LCIC fractalkine expression. A freehand tool with a line thickness of 100μm was used to sample and fully encompass layer 2 GAD-positive modules in a ventral-to-dorsal progression. Once the sampling contour was set, a region of interest (ROI) function was utilized to duplicate and save the exact sampling

contour for use in the other channel of the same image. Sampling data for the two channels (green: GAD, red: CX3CL1) provided a brightness profile pattern of the two fluorescent markers with respect to each other. Representative signal waveforms showed clear overlap in brightness peaks and troughs, suggesting alignment of CX3CL1 patterning at P12 with GAD-defined modules.

2.6. Quantification of MGC densities and LCIC location

JPEG2000 file format images throughout the caudorostral extent of the observed LCIC modularity were selected and opened in NIS-Elements software. Three animals were used in the quantitative analyses at each of the five ages and each of the genotypes (i.e. 6 mice at each age for a total of 30 mice). For each mouse, multiple sections (a minimum of 3) were sampled in order to capture anatomical variability at different levels of the LCIC. Thus, at least 9 sections from a minimum of 3 animals were included for each category in the statistical analyses. After defining contiguous GAD-positive modular zones as described above, the measurement tool for area was utilized to draw encompassing boundaries around the LCIC and its modules. Area was calculated using the area tool under the measurement dropdown. To calculate total volumetric LCIC MGC density, all MGCs within the LCIC outline were counted using the count function, then divided by the area multiplied by the number of steps minus 1 and step size of the Z-series (volumetric $MGC\ \ density\ \ =\ \ \frac{\#\ \ of\ \ MGCs}{area\ \ (\#\ \ of\ \ z\ \ step\ \ -\ \ 1)(step\ \ size)}$). Next, MGCs were plotted as either residing within or outside of LCIC modular zones. MGCs were determined to be within a module if the entire soma was housed inside the modular confine as previously defined with the freehand area tool. Modular area was subtracted from total LCIC area to define modular versus extramodular matrix area. To make statistical comparisons between overall MGC density at the examined developmental stages for each genotype, as well as between MGC location (modular vs. matrix), independent, two-tailed sample t-tests, assuming equal variance (Type 2) were run after passing a Shapiro-Wilk test for normality ($p > 0.05$), with statistical significance defined as $p < 0.05$.

3. RESULTS

3.1. Microglial cell presence and patterning in the nascent LCIC

To examine MGC colonization of the neonatal LCIC with respect to its emerging compartmental arrangement, Iba1 (a MGC-specific ionized calcium-binding adaptor protein) immunostaining was performed in a developmental series of GAD67-GFP mice. At birth, MGCs are present in all subdivisions of the IC (Figure 3a–c, arrowheads in b). GAD-positive modules are not yet defined at this age, nor is there any apparent MGC organization. By P4, MGCs chiefly reside in layer 2 of the LCIC and begin to localize to emerging modular borders as GAD-positive patches become increasingly evident (Figure 3d–f, dashed contours). Concurrent with the peak of the LCIC critical period at P8, Iba1-positive MGCs are predominately found encompassing modular-matrix boundaries (Figure 3g–i). At P12, when segregation of LCIC afferents into their modality-specific compartments is largely complete, MGCs invade and concentrate within GAD-defined modular zones, known to be richly innervated by somatosensory terminals (Figure 3j–l). Shortly after hearing onset and

the closure of the defined LCIC critical period (P16), MGCs exhibit a more homogenous or even distribution throughout the IC (Figure 3m–o). Taken together, this developmental progression reveals an increasing density of MGCs in the LCIC from birth to P12, as well as MGC entry of modular confines that coincides with the establishment of LCIC fine structure and its interfacing connectivity maps.

3.2. Validation of CX3CR1-GFP mouse line and extent of CX3CR1/Iba1 co-localization

In a variety of systems fractalkine signaling (CX3CL1-CX3CR1) is important not only for the initial recruitment of MGCs to a given brain structure, but also for regulating MGC entry into discrete target zones undergoing active circuit assembly/remodeling (Hoshiko, Arnoux, Avignone, Yamamoto, & Audinat, 2012; Zhan et al., 2014). To investigate the potential involvement of fractalkine-mediated MGC recruitment to, and migration within the LCIC, CX3CR1-GFP knock-in mice were utilized (i.e. CX3CR1 gene replaced with a GFP reporter; Jung et al., 2000). MGCs in both heterozygous ($CX3CR1^{+/GFP}$) and homozygous ($CX3CR1^{GFP/GFP}$) animals express EGFP under the control of CX3CR1 expression. Whereas MGCs in $CX3CR1^{GFP/GFP}$ mice completely lack CX3CR1 and are thereby rendered incapable of fractalkine signaling, comparable *in vivo* findings in $CX3CR1^{+/GFP}$ and Iba1-GFP mice regarding various microglial assessments suggest heterozygotes retain the ability for functional signaling (Paolicelli, Bisht, & Tremblay, 2014; Hirasawa et al., 2005). To validate MGC-specific GFP expression in the postnatal IC we performed immunostaining for Iba1 in a developmental series of CX3CR1 heterozygous mice (Figure 4a–e). CX3CR1-GFP expression co-localized with Iba1 immunostaining both in microglial cell bodies and proximal processes. Iba1 expression was also evident clear into distal, fine processes. These results verify that the CX3CR1-GFP knock-in mouse line selectively labels MGCs in the neonatal midbrain. Further analyses of the extent of CX3CR1/Iba1 overlap revealed that while all Iba1-positive MGCs also express the fractalkine receptor at each of the examined ages, on average only 19.2% of CX3CR1-positive microglia were also positive for Iba1 across this developmental timespan (SEM = 3.36%, CV_{mean} = 17.5%). Such findings suggest that multiple MGC subpopulations exist in the postnatal LCIC with different expression signatures that perhaps serve unique developmental roles. Increased MGC process ramification was reliably observed at later timepoints (Figure 4a, e; P12, P16 respectively). Such morphological changes have been linked to shifts in activation states (Heindl et al., 2018; Li & Barres, 2018; Young & Morrison, 2018), suggesting that LCIC MGCs may transition to morphologies in keeping with resting or surveilling states as its critical period comes to a close.

3.3. Fractalkine signaling controls MGC entry into LCIC modular zones

To assess the functional importance of fractalkine receptor signaling on MGC colonization of the LCIC and occupancy of its emerging compartments, CX3CR1-GFP tissue (WT, heterozygous, homozygous) was immunostained for GAD67 (LCIC modular marker) and compared. A similar developmental pattern was observed in both $CX3CR1^{+/+}$ and $CX3CR1^{+/GFP}$ mice at each of the examined ages and was consistent with Iba1 findings. Thus, heterozygous results are presented alongside age-matched homozygous signaling mutants in Figure 5. At birth, CX3CR1-expressing MGCs are modest in number, yet present throughout the IC (Figure 5a, f, arrowheads). At P4, few MGCs are observed within

emerging LCIC modular zones, with the vast majority residing either in the surrounding matrix or directly ringing developing modular-extramodular boundaries (Figure 5b, g). Such MGC positioning bias is even more apparent at P8, as MGCs preferentially occupy the extramodular matrix clear up to its now distinctly demarcated modular borders (Figure 5c, h). Whereas microglia reliably enter modular fields at P12 in mice with functional signaling (Figure 5d), similar occupancy at this timepoint was consistently not observed in mice lacking functional fractalkine receptors (Figure 5i). This disparity was transient, however, as MGCs in CX3CR1$^{GFP/GFP}$ mice reliably invade modular centers by P16 (Figure 5j), exhibiting more homogeneous distributions comparable to their heterozygous littermates (Figure 5e, j). Qualitative observations suggest MGC numbers steadily increase in the LCIC over the first 1–2 postnatal weeks in both CX3CR1$^{+/GFP}$ and CX3CR1$^{GFP/GFP}$ mice.

To further assess CX3CL1/CX3CR1 involvement in MGC colonization of the nascent LCIC and their subsequent occupancy of modular zones, we quantified MGC densities for CX3CR1$^{+/GFP}$ and CX3CR1$^{GFP/GFP}$ mice (at each developmental stage, as well as for its emerging compartments [i.e. modular *vs.* matrix]). We also performed CX3CL1 staining in GAD67-GFP mice to determine if fractalkine expression follows a similar progression to that described in barrel cortex (Hoshiko, Arnoux, Avignone, Yamamoto, & Audinat, 2012), namely discrete compartmental expression just prior to MGC occupancy.

3.4. MGC density differences in CX3CR1 signaling mutants

MGC densities increased steadily over the examined LCIC critical period (P0-P12) for both genotypes before a reduction was observed at P16 (Figure 6a). At P4 and P8, MGC density in CX3CR1$^{+/GFP}$ mice is significantly greater than that of CX3CR1$^{GFP/GFP}$ littermates. This difference at the peak critical period is not sustained, as no statistical difference is observed at P12. Interestingly, genotypic differences were once again observed after critical period closure (P16). Consistent with qualitative findings, significantly more MGCs occupy modular zones at P12 in CX3CR1$^{+/GFP}$ mice as compared to CX3CR1$^{GFP/GFP}$ mice (Figure 6b). By P16, MGCs exhibit a rather homogenous distribution throughout the LCIC, confirming a transient delay of migration into modular zones in the absence of functional fractalkine receptor signaling.

3.5. Fractalkine (CX3CL1) expression in the developing LCIC

At birth, neuronal fractalkine expression is present in the LCIC albeit sparse (Figure 7a, b). At P4 and P8, CX3CL1 expression continues to be unremarkable, though somewhat biased to dorsal aspects of the LCIC (Figure 7c–f). By P12, there is an appreciable shift in CX3CL1 expression, now highly localized to neuronal populations within modular zones (Figure 7g, h). Modular GAD-positive neurons rarely co-localize with fractalkine-expressing cells, suggesting the vast majority of CX3CL1-positive neurons are non-GABAergic. After critical period closure, fractalkine expression becomes homogeneously distributed throughout the IC (including the LCIC; Figure 7i, j), similar to that previously reported in all layers of somatosensory cortex at a similar post-shaping developmental timepoint (P30; Hoshiko, Arnoux, Avignone, Yamamoto, & Audinat, 2012).

Once LCIC compartmentalization is set and afferent arrays are largely segregated at P12, CX3CL1 layer 2 expression is highly concentrated to GAD-defined modular zones (Figure 8a–c). This discrete expression pattern coincides with MGC invasion of modular zones in CX3CR1$^{+/GFP}$ mice, suggesting that fractalkine upregulation signals the entry of surrounding CX3CR1-expressing microglia. CX3CL1- and GAD-positve cell populations within LCIC modules are largely distinct (Figure 8d–f), suggesting the majority of fractalkine expressing neurons are likely excitatory in nature. Brightness profiles generated from identical ROI layer 2 sampling of both channels reveal fluctuating signal waveforms at P12 that are remarkably in-phase with each other, further supporting modular fractalkine expression at this critical timepoint (Figure 9a, b).

4. DISCUSSION

The present experiments implicate MGCs in midbrain development and provide insights regarding potential mechanisms underlying multimodal LCIC compartmentalization and circuitry refinement. The results provide the first description of MGC presence in the nascent LCIC, dynamic changes in their patterning over an early critical period, as well as an initial assessment of fractalkine-mediated MGC recruitment into the LCIC and its defined compartmental zones. Findings are largely in keeping with CX3CL1-CX3CR1 signaling previously established in other unimodal systems of developing mouse and rat concerning MGC recruitment and initial patterning (Fiske & Brunjes, 2000; Schafer et al., 2012; Hoshiko, Arnoux, Avignone, Yamamoto, & Audinat, 2012; Nayak, Roth, & McGavern, 2014; Miyamoto et al., 2016). Our findings suggest similar microglial roles are likely at play in multimodal LCIC circuit assembly and refinement. MGCs have colonized the midbrain by birth and soon after appear to recognize emerging boundaries of its characteristic modular-matrix framework. Fractalkine (CX3CL1) is a known chemotactic signal for recruiting fractalkine receptor (CX3CR1)-expressing MGCs to the site of action (Paolicelli, Bisht, & Tremblay, 2014). Our results implicate CX3CL1-CX3CR1 signaling in overall MGC recruitment to the LCIC itself, as well as regulating subsequent entry into modular confines at P12.

4.1. MGCs in the developing LCIC and other discretely-organized systems

Our Iba1 staining and work in CX3CR1-GFP mice provide evidence of MGC presence during the early postnatal period of LCIC shaping. During this time MGCs bias to layer 2 of the LCIC before the peak period of shaping for emerging multisensory maps. Usually by P4, and certainly by P8, microglia surround emergent modules prior to invading modular confines by P12 (Figure 10). MGCs exhibit a homogeneous distribution throughout the IC by P16, with seemingly more ramified morphological appearances than at earlier postnatal stages, perhaps suggestive of a recent switch to resting or surveilling states (Nayak, Roth, & McGavern, 2014).

We hypothesized fractalkine (CX3CL1) might signal the observed MGC behaviors of our initial experiments, namely recruitment to the LCIC and temporal control of entry into discrete modular domains. In the whisker-related barrel fields of somatosensory cortex, CX3CL1 expression is temporally upregulated in barrel centers and important for regulating

CX3CR1-expressing MGC invasion of these domains during the critical period for shaping of its thalamocortical inputs (Hoshiko, Arnoux, Avignone, Yamamoto, & Audinat, 2012). Utilizing the same CX3CR1-GFP mouse line, we report several analogous findings in the LCIC. First, patchy fractalkine expression is transient and overlaps newly established compartments in time to signal MGC occupancy. Second, we show a similar delay or lag of MGC entry into modules in $CX3CR1^{GFP/GFP}$ signaling mutants. Finally, at P12 when MGCs have invaded modules in $CX3CR1^{+/GFP}$ but not $CX3CR1^{GFP/GFP}$ mice, comparable overall LCIC MGC densities are observed for both genotypes, in keeping with that reported at an equivalent timepoint in barrel cortex (P7, Hoshiko, Arnoux, Avignone, Yamamoto, & Audinat, 2012). The question as to why MGCs avoid entering LCIC modules prior to P12 remains unanswered. It is likely signaling mechanisms other than CX3CL1-CX3CR1 interactions are responsible for regulating this initial step, as a deficiency in fractalkine receptors does not influence initial MGC patterning around emerging LCIC modules. As evidenced by recent single-cell resolution RNA sequencing studies (Hammond et al., 2019; Masuda et al., 2019; Tan, Yuan, & Tian, 2020), distinct subpopulations of microglia are present throughout the brain across the lifespan and in response to injury and inflammation. Such MGC heterogeneity is especially true during early critical periods of development. Preliminary findings presented here seem to support this notion as different MGC markers appear to highlight different subpopulations (e.g. only 19.2% of CX3CR1-positive microglia were also positive for Iba1 over the examined developmental period). It will be important to explore how many clusters of microglia with different genetic profiles interact with resident LCIC neurons (as well as other glial) and their developing networks, and whether each serve unique roles and responsibilities.

Beyond the above-mentioned similarities with barrel cortex concerning specific recruitment to discrete target zones, the present data also parallel findings in other brain structures where fractalkine signaling mediates timely MGC colonization. Here, we show a slower increase of MGC density from P4 to P8 in $CX3CR1^{GFP/GFP}$ mice compared to $CX3CR1^{+/GFP}$ littermates. Analogous transient impairments occur in CX3CR1 deficient mice in the CA1 region of hippocampus between P8 and P28 (Paolicelli et al., 2011). Motor cortex exhibits similar reductions in MGC density at P5 in mice with compromised fractalkine signaling, due to increased accumulation of microglia in the subcortical white matter (Ueno et al., 2013). Taken together, our data support the notion that at the earliest postnatal stages fractalkine may serve as a more global chemokine, recruiting microglia into the IC itself and the LCIC proper. Once LCIC compartments are established and multimodal afferents are largely segregated (Dillingham, Gay, Behrooz, & Gabriele, 2017; Gay, Brett, Stinson, & Gabriele, 2018; Lamb-Echegaray, Noftz, Stinson, & Gabriele, 2019; Stinson, Brett, Carroll, & Gabriele, 2021), it seems fractalkine signaling may exert more local influences, regulating entry into specific zones. It remains to be determined whether after advancing into modules MGCs selectively remove underutilized synapses (e.g. C3 “eat me tag;” Schafer et al., 2012; Schafer & Stevens, 2015), or perhaps aid in the maturation of contacts opsonized for sparing (e.g. CD47 “don’t eat me;” Lehrman et al., 2018).

4.2. Fractalkine in the multimodal LCIC and potential behavioral implications

Fractalkine signaling plays an important role regulating plasticity of neural circuits during normal development and has functional consequences on behavior, learning, and memory (Paolicelli, Bisht, & Tremblay, 2014). Compromised fractalkine signaling in mice leads to deficits in synaptic pruning (specifically excess weak excitatory contacts), as well as impaired social interaction and increased repetitive behaviors associated with ASD and other neurodevelopmental conditions (Paolicelli et al., 2011; Zhan et al., 2014). Recent studies show that while LCIC multimodal maps appear segregated by P12 (Lamb-Echegaray, Noftz, Stinson, & Gabriele, 2019), an intrinsic connectivity exists allowing for unidirectional flow from the matrix (auditory) into the modules (somatosensory; Lesicko, Sons, & Llano, 2020). Such connections could provide the anatomical substrate underlying multisensory LCIC response properties (Aitkin, Kenyon, & Philpott, 1981; Gruters & Groh, 2012). It seems the LCIC may serve as an important parallel processing hub where different information streams allow for both the continued segregation, as well as the initial integration of unimodal inputs (Lesicko, Sons, & Llano, 2020), before being sent on for higher order processing. Indeed, the LCIC is not only critical for auditory reflexive and orientation behaviors, as it figures prominently as a modulator of the acoustic startle response (Groves, Wilson, & Boyle, 1974; Leitner & Cohen, 1985; Parham & Willott, 1990), but also in multisensory enhancement of such responses as it sends robust projections to deep aspects of the superior colliculus (Lesicko, Sons, & Llano, 2020). CX3CR1 deficiency influences the maturation of inhibitory contacts at the level of the auditory brainstem and significantly reduces ABR peak latencies (Milinkeviciute, Chokr, Castro, & Cramer, 2021). It remains to be seen if MGC function and fractalkine signaling are equally critical for establishing a balance of excitatory/inhibitory connections and selective pruning of emerging neural maps in the multimodal LCIC. Our data show very little LCIC neuronal colocalization of CX3CL1and GAD expression. It will be interesting to see if deficiencies in fractalkine signaling influence the selective pruning and/or maturation of excitatory LCIC synapses as has been described in other burgeoning structures (Paolicelli et al., 2011; Zhan et al., 2014). If so, signaling mutants might exhibit consequences in multisensory processing tasks (e.g. multisensory binding) that are highly predictive of onset and severity of certain neurodevelopmental disorders due to unrefined LCIC map configurations. Perhaps compromised parallel processing through the LCIC due to MGC dysfunction might help explain why sensory processing in ASD is often selectively biased towards unimodal details of the perceptual world at the expense of the larger whole.

4.3. Concluding Remarks

Understanding the importance of MGC-neuronal interplay and fractalkine signaling in the development of LCIC modularity should ultimately provide additional insights concerning the developmental mechanisms that shape multisensory circuits, as well as the consequences that result if such connections are not appropriately refined during early critical periods. Taken together, our data implicate MGCs in orchestrating critical aspects of LCIC development and provide compelling reasons for continued experimentation aimed at identifying the precise mechanisms whereby MGCs exert their varied influences.

ACKNOWLEDGEMENTS

The authors would like to sincerely thank Dr. Kristopher Kubow for his microscopy expertise and oversight of the James Madison University Light Microscopy and Imaging Facility.

FUNDING

This work was supported by the National Institutes of Health (DC018885-01), the National Science Foundation (DBI-0619207, DBI-1725855), and the James Madison University Light Microscopy and Imaging Facility.

DATA AVAILABILITY STATEMENT

The raw data and datasets generated for this study will be made available upon reasonable request by the corresponding author.

REFERENCES

Ainsworth K, Ostrolenk A, Irion C, & Bertone A (2021). Reduced multisensory facilitation exists at different periods of development in autism. Cortex 134, 195–206. doi: 10.1016/j.cortex.2020.09.031. [PubMed: 33291045]

Aitkin LM, Kenyon CE, & Philpott P (1981). The representation of the auditory and somatosensory systems in the external nucleus of the cat inferior colliculus. Journal of Comparative Neurology 196, 25–40. doi: 10.1002/cne.901960104.

Allen NJ, & Lyons DA (2018). Glia as architects of central nervous system formation and function. Science 362, 181–185. doi: 10.1126/science.aat0473. [PubMed: 30309945]

Chernock ML, Larue DT, & Winer JA (2004). A periodic network of neurochemical modules in the inferior colliculus. Hearing Research 188, 12–20. doi: 10.1016/S0378-5955(03)00340-X. [PubMed: 14759566]

Collignon O, Charbonneau G, Peters F, Nassim M, Lassonde M, Lepore F, … Bertone A (2013). Reduced multisensory facilitation in persons with autism. Cortex 49, 1704–1710. doi: 10.1016/j.cortex.2012.06.001. [PubMed: 22818902]

Cramer KS, & Gabriele ML (2014). Axon guidance in the auditory system: Multiple functions of Eph receptors. Neuroscience 277, 152–162. doi: 10.1016/j.neuroscience.2014.06.068. [PubMed: 25010398]

Dillingham CH, Gay SM, Behrooz R, & Gabriele ML (2017). Modular-extramodular organization in developing multisensory shell regions of the mouse inferior colliculus. Journal of Comparative Neurology 525, 3742–3756. doi: 10.1002/cne.24300.

Fiske BK, & Brunjes PC (2000). Microglial activation in the developing rat olfactory bulb. Neuroscience 96, 807–815. doi: 10.1016/s0306-4522(99)00601-6. [PubMed: 10727798]

Frick LR, Williams K, & Pittenger C (2013). Microglial dysregulation in psychiatric disease. Clinical and Developmental Immunology 2013, 608654. doi: 10.1155/2013/608654. [PubMed: 23690824]

Frost JL, & Schafer DP (2016). Microglia: Architects of the developing nervous system. Trends in Cell Biology 26, 587–597. doi: 10.1016/j.tcb.2016.02.006. [PubMed: 27004698]

Gabriele ML, Brubaker DQ, Chamberlain KA, Kross KM, Simpson NS, & Kavianpour SM (2011). EphA4 and ephrin-B2 expression patterns during inferior colliculus projection shaping prior to experience. Developmental Neurobiology 71, 182–199. doi: 10.1002/dneu.20842. [PubMed: 20886601]

Gay SM, Brett CA, Stinson JPC, & Gabriele ML (2018). Alignment of EphA4 and ephrin-B2 expression patterns with developing modularity in the lateral cortex of the inferior colliculus. Journal of Comparative Neurology 526, 2706–2721. doi: 10.1002/cne.24525.

Ginhoux F, Lim S, Hoeffel G, Low D, & Huber T (2013). Origin and differentiation of microglia. Frontiers in Cellular Neuroscience, 7, 45. doi: 10.3389/fncel.2013.00045. [PubMed: 23616747]

Groves PM, Wilson CJ, & Boyle RD (1974). Brain stem pathways, cortical modulation, and habituation of the acoustic startle response. Behavioral Biology. 10, 391–418. doi: 10.1016/s0091-6773(74)91975-0. [PubMed: 4832941]

Gruters KG, & Groh JM (2012). Sounds and beyond: multisensory and other non-auditory signals in the inferior colliculus. Frontiers in Neural Circuits 6, 96. doi: 10.3389/fncir.2012.00096. [PubMed: 23248584]

Gunner G, Cheadle L, Johnson KM, Ayata P, Badimon A, Mondo E, … Schafer DP (2019). Sensory lesioning induces microglial synapse elimination via ADAM10 and fractalkine signaling. Nature Neuroscience 22, 1075–1088. doi: 10.1038/s41593-019-0419-y. [PubMed: 31209379]

Hammond TR, Dufort C, Dissing-Olesen L, Giera S, Young A, Wysoker A, … Stevens B (2019). Single-cell RNA sequencing of microglia throughout the mouse lifespan and in the injured brain reveals complex cell-state changes. Immunity 50, 253–271.e6. doi: 10.1016/j.immuni.2018.11.004. [PubMed: 30471926]

Heindl S, Gesierich B, Benakis C, Llovera G, Duering M, & Liesz A (2018). Automated morphological analysis of microglia after stroke.. Frontiers in Cellular Neuroscience 12, 106. doi: 10.3389/fncel.2018.00106. [PubMed: 29725290]

Hirasawa T, Ohsawa K, Imai Y, Ondo Y, Akazawa C, Uchino S, & Kohsaka S (2005). Visualization of microglia in living tissues using Iba1-EGFP transgenic mice. Journal of Neuroscience Research 81, 357–62. doi: 10.1002/jnr.20480. [PubMed: 15948177]

Hong S, Dissing-Olesen L, & Stevens B (2016). New insights on the role of microglia in synaptic pruning in health and disease. Current Opinion in Neurobiology 36, 128–134. doi: 10.1016/j.conb.2015.12.004. [PubMed: 26745839]

Hoshiko M, Arnoux I, Avignone E, Yamamoto N, & Audinat E (2012). Deficiency of the microglial receptor CX3CR1 impairs postnatal functional development of thalamocortical synapses in the barrel cortex. Journal of Neuroscience 32, 15106–15111. doi: 10.1523/jneurosci.1167-12.2012. [PubMed: 23100431]

Jung S, Aliberti J, Graemmel P, Sunshine MJ, Kreutzberg GW, Sher A, & Littman DR (2000). Analysis of fractalkine receptor CX(3)CR1 function by targeted deletion and green fluorescent protein reporter gene insertion. Molecular and Cellular Biology 20, 4106–4114. doi: 10.1128/mcb.20.11.4106-4114.2000. [PubMed: 10805752]

Lamb-Echegaray ID, Noftz WA, Stinson JPC, & Gabriele ML (2019). Shaping of discrete auditory inputs to extramodular zones of the lateral cortex of the inferior colliculus. Brain Structure and Function 224, 3353–3371. doi: 10.1007/s00429-019-01979-6. [PubMed: 31729553]

Lehrman EK, Wilton DK, Litvina EY, Welsh CA, Chang ST, Frouin A, … Stevens B (2018). CD47 protects synapses from excess microglia-mediated pruning during development. Neuron 100, 120–134.e6. doi: 10.1016/j.neuron.2018.09.017. [PubMed: 30308165]

Leitner DS, & Cohen ME (1985). Role of the inferior colliculus in the inhibition of acoustic startle in the rat. Physiology & Behavior 34, 65–70. doi: 10.1016/0031-9384(85)90079-4. [PubMed: 4034696]

Lesicko AMH, Hristova TS, Maigler KC, & Llano DA (2016). Connectional modularity of top-down and bottom-up multimodal inputs to the lateral cortex of the mouse inferior colliculus. Journal of Neuroscience 36, 11037–11050. doi: 10.1523/jneurosci.4134-15.2016. [PubMed: 27798184]

Lesicko AMH, Sons SK, & Llano DA (2020). Circuit mechanisms underlying the segregation and integration of parallel processing streams in the inferior colliculus. Journal of Neuroscience 40, 6328–6344. doi: 10.1523/jneurosci.0646-20.2020. [PubMed: 32665405]

Li Q, & Barres BA (2018). Microglia and macrophages in brain homeostasis and disease. Nature Reviews Immunology, 18, 225–242. doi: 10.1038/nri.2017.125.

Luo L, & Flanagan JG (2007). Development of continuous and discrete neural maps. Neuron 56, 284–300. doi: 10.1016/j.neuron.2007.10.014. [PubMed: 17964246]

Masuda T, Sankowski R, Staszewski O, Böttcher C, Amann L, Sagar, … Prinz M. (2019). Spatial and temporal heterogeneity of mouse and human microglia at single-cell resolution. Nature 566, 388–392. doi: 10.1038/s41586-019-0924-x. [PubMed: 30760929]

Milinkeviciute G, Chokr SM, Castro EM, & Cramer KS (2021). CX3CR1 mutation alters synaptic and astrocytic protein expression, topographic gradients, and response latencies in the auditory brainstem. Journal of Comparative Neurology 529, 3076–3097. doi: 10.1002/cne.25150.

Miyamoto A, Wake H, Ishikawa AW, Eto K, Shibata K, Murakoshi H, … Nabekura J (2016). Microglia contact induces synapse formation in developing somatosensory cortex. Nature Communications 7, 12540. doi: 10.1038/ncomms12540.

Mizutani M, Pino PA, Saederup N, Charo IF, Ransohoff RM, & Cardona AE (2012). The fractalkine receptor but not CCR2 is present on microglia from embryonic development throughout adulthood. Journal of Immunology 188, 29–36. doi: 10.4049/jimmunol.1100421.

Nayak D, Roth TL, & McGavern DB (2014). Microglia development and function. Annual Review of Immunology 32, 367–402. doi: 10.1146/annurev-immunol-032713-120240.

Paolicelli RC, Bisht K, & Tremblay MÈ (2014). Fractalkine regulation of microglial physiology and consequences on the brain and behavior. Frontiers in Cellular Neuroscience 8, 129. doi: 10.3389/fncel.2014.00129. [PubMed: 24860431]

Paolicelli RC, Bolasco G, Pagani F, Maggi L, Scianni M, Panzanelli P, … Gross CT (2011). Synaptic pruning by microglia is necessary for normal brain development. Science 333, 1456–1458. doi: 10.1126/science.1202529. [PubMed: 21778362]

Parham K, & Willott JF (1990). Effects of inferior colliculus lesions on the acoustic startle response. Behavioral Neuroscience 104, 831–840. doi: 10.1037//0735-7044.104.6.831. [PubMed: 2285482]

Schafer DP, Lehrman EK, Kautzman AG, Koyama R, Mardinly AR, Yamasaki R, … Stevens B (2012). Microglia sculpt postnatal neural circuits in an activity and complement-dependent manner. Neuron 74, 691–705. doi: 10.1016/j.neuron.2012.03.026. [PubMed: 22632727]

Schafer DP, & Stevens B (2015). Microglia function in central nervous system development and plasticity. Cold Spring Harbor Perspectives in Biology 7, a020545. doi: 10.1101/cshperspect.a020545. [PubMed: 26187728]

Squarzoni P, Oller G, Hoeffel G, Pont-Lezica L, Rostaing P, Low D, … Garel S (2014). Microglia modulate wiring of the embryonic forebrain. Cell Reports 8, 1271–1279. doi: 10.1016/j.celrep.2014.07.042. [PubMed: 25159150]

Stinson JPC, Brett CA, Carroll JB, & Gabriele ML (2021). Registry of compartmental ephrin-B3 patterns with respect to emerging multimodal midbrain maps. Frontiers in Neuroanatomy 15, 649478. doi: 10.3389/fnana.2021.649478. [PubMed: 33815071]

Stevenson RA, Segers M, Ferber S, Barense MD, & Wallace MT (2014). The impact of multisensory integration deficits on speech perception in children with autism spectrum disorders. Frontiers in Psychology 5, 379. doi: 10.3389/fpsyg.2014.00379. [PubMed: 24904448]

Stevenson RA, Siemann JK, Schneider BC, Eberly HE, Woynaroski TG, Camarata SM, & Wallace MT (2014a). Multisensory temporal integration in autism spectrum disorders. Journal of Neuroscience 34, 691–697. doi: 10.1523/jneurosci.3615-13.2014. [PubMed: 24431427]

Stevenson RA, Siemann JK, Woynaroski TG, Schneider BC, Eberly HE, Camarata SM, & Wallace MT (2014b). Evidence for diminished multisensory integration in autism spectrum disorders. Journal of Autism and Developmental Disorders 44, 3161–3167. doi: 10.1007/s10803-014-2179-6. [PubMed: 25022248]

Tamamaki N, Yanagawa Y, Tomioka R, Miyazaki J, Obata K, & Kaneko T (2003). Green fluorescent protein expression and colocalization with calretinin, parvalbumin, and somatostatin in the GAD67-GFP knock-in mouse. Journal of Comparative Neurology 467, 60–79. doi: 10.1002/cne.10905.

Tan YL, Yuan Y, & Tian L (2020). Microglial regional heterogeneity and its role in the brain. Molecular Psychiatry 25, 351–367. doi: 10.1038/s41380-019-0609-8. [PubMed: 31772305]

Tay TL, Savage JC, Hui CW, Bisht K, & Tremblay MÈ (2017). Microglia across the lifespan: from origin to function in brain development, plasticity and cognition. Journal of Physiology 595, 1929–1945. doi: 10.1113/JP272134.

Thion MS, & Garel S (2017). On place and time: microglia in embryonic and perinatal brain development. Current Opinion in Neurobiology 47, 121–130. doi: 10.1016/j.conb.2017.10.004. [PubMed: 29080445]

Thion MS, Ginhoux F, & Garel S (2018). Microglia and early brain development: An intimate journey. Science 362, 185–189. doi: 10.1126/science.aat0474. [PubMed: 30309946]

Tremblay MÈ, Stevens B, Sierra A, Wake H, Bessis A, & Nimmerjahn A (2011). The role of microglia in the healthy brain. Journal of Neuroscience 31, 16064–16069. doi: 10.1523/jneurosci.4158-11.2011. [PubMed: 22072657]

Ueno M, Fujita Y, Tanaka T, Nakamura Y, Kikuta J, Ishii M, & Yamashita T (2013). Layer V cortical neurons require microglial support for survival during postnatal development. Nature Neuroscience 16, 543–551. doi: 10.1038/nn.3358. [PubMed: 23525041]

Wallace MM, Harris JA, Brubaker DQ, Klotz CA, & Gabriele ML (2016). Graded and discontinuous EphA-ephrinB expression patterns in the developing auditory brainstem. Hearing Research 335, 64–75. doi: 10.1016/j.heares.2016.02.013. [PubMed: 26906676]

Young K, & Morrison H (2018). Quantifying microglia morphology from photomicrographs of immunohistochemistry prepared tissue using ImageJ. Journal of Visualized Experiments 136, 57648. doi: 10.3791/57648.

Zhan Y, Paolicelli RC, Sforazzini F, Weinhard L, Bolasco G, Pagani F, … Gross CT (2014). Deficient neuron-microglia signaling results in impaired functional brain connectivity and social behavior. Nature Neuroscience 17, 400–406. doi: 10.1038/nn.3641. [PubMed: 24487234]

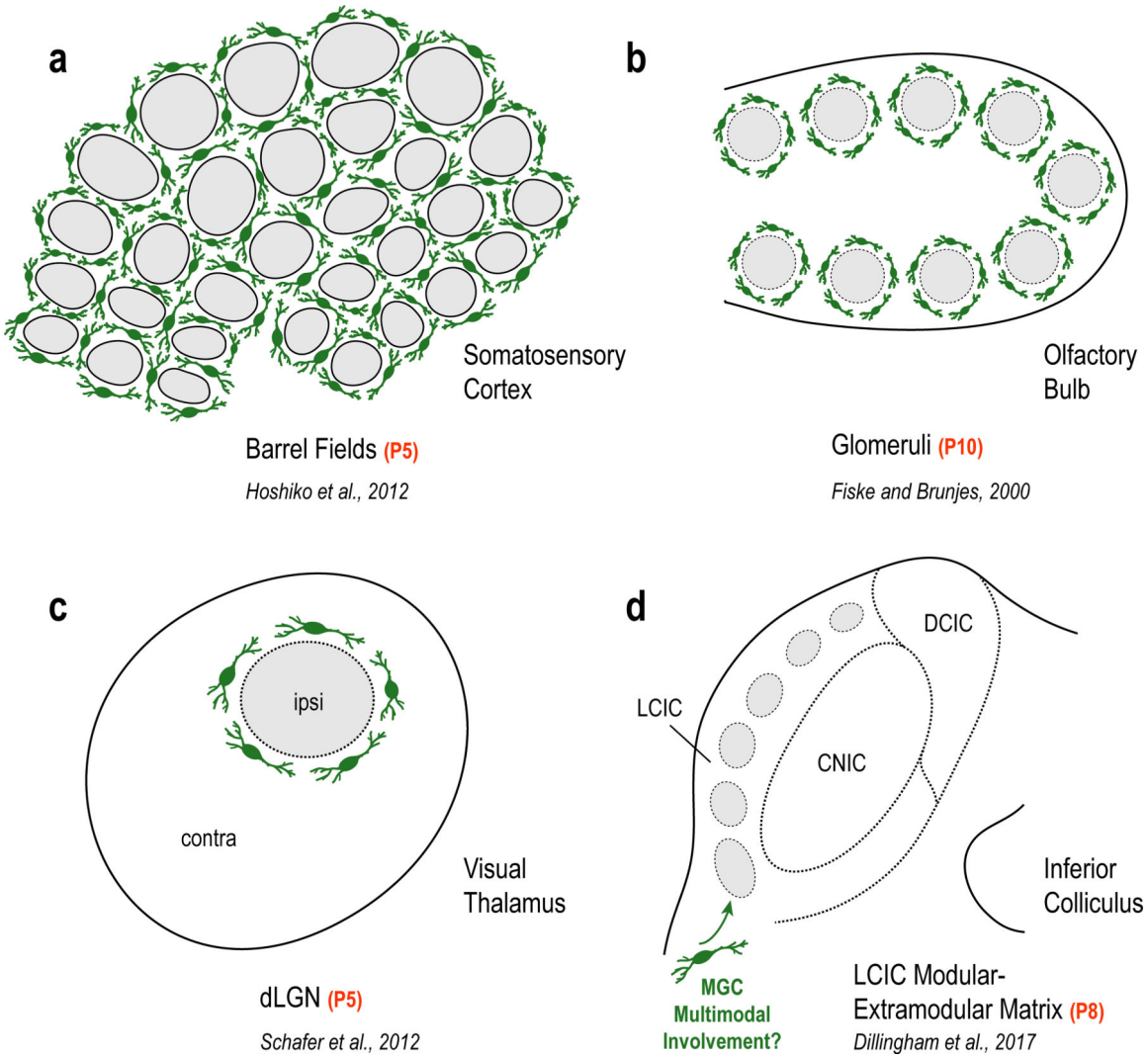

Figure 1.

Characteristic MGC patterns in unimodal systems of barrel cortex (a), olfactory bulb (b), and visual thalamus (c) encompassing discrete compartments just prior to peak critical periods of synaptic pruning and circuit refinement. Microglial involvement in shaping similar discretely-organized multimodal maps (e.g. LCIC modular-extramodular matrix) has yet to be examined (d).

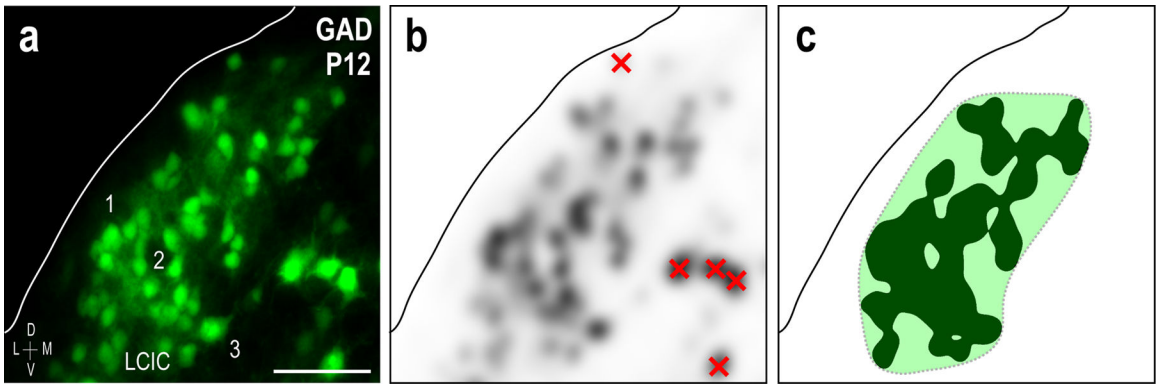

Figure 2.

Methods for objective identification of LCIC layer 2 GAD-positive modules. GAD-GFP LCIC labeling from a representative P12 mouse (a). After conversion to grayscale, GAD channels were smoothed with a Gaussian filter (radius = 20.0 pixels), and inverted (b). GAD-positive cells in layers 1 and 3 were subtracted (red x's in b) prior to applying a threshold function (level: 200). Adjoining layer 2 domains (solid fill) were then best fit with smoothed contours (dashed) to define modular boundaries (c). Scale bar in (a) = 50μm.

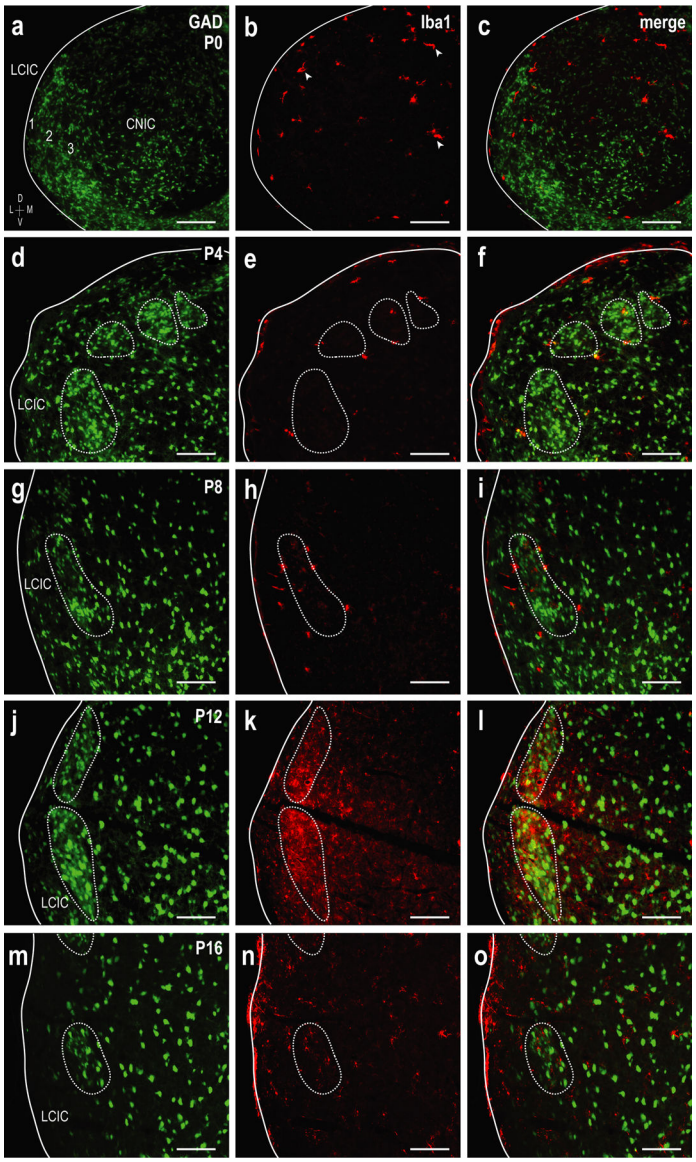

Figure 3.

Developmental progression of Iba1 expression showing MGCs (red) with emerging LCIC GAD-positive modules (green) at P0 (a-c), P4 (d-f), P8 (g-i), P12 (j-l), and P16 (m-o). At birth, MGCs are present in all IC subdivisions (arrowheads in b). At this age, GAD-positive modules are not readily apparent and MGCs are sporadic, not appearing to be organized in any specific manner. By P4, GAD modules become evident and MGCs are largely localized to the LCIC, namely occupying layer 2 and beginning to localize to modular borders (dashed contours). At P8, the vast majority of microglia are positioned in close proximity to modular-matrix boundaries, before invading modular confines at P12. At P16, MGCs are more homogeneously distributed throughout the LCIC, occupying both modular zones and the surrounding matrix. The density of Iba1-positive microglia increases steadily over the early postnatal period and appears to peak at P12. Scale bars = 100μm.

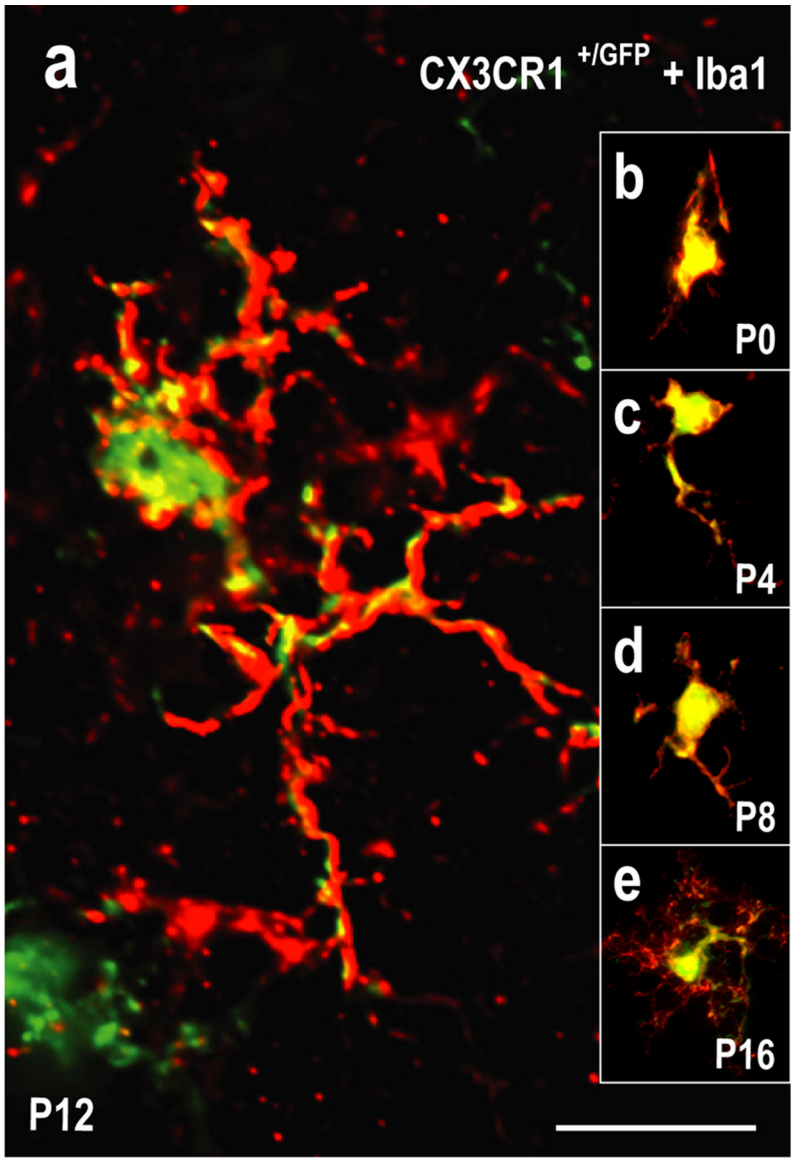

Figure 4.

Co-localization of fractalkine receptor-GFP microglial expression in the LCIC with Iba1 (an established microglial marker) in a developmental series (P0, P4, P8, P12, P16) of CX3CR1$^{+/GFP}$ mice. High magnification flattened z-stacks at each developmental stage (a-e) verifying fractalkine receptor (CX3CR1) expression (green) is specific to MGCs, colocalizing with Iba1 (red) in the LCIC. While all Iba1-positive MGCs were also positive for CX3CR1, not all CX3CR1-positive MGCs were also positive for Iba1 (19.2% over the examined developmental period). MGC ramification appears increasingly complex with age, with elaborate processes consistently seen at P12 (a) and P16 (e). Such morphological changes may speak towards a shift in MGC activation states as the LCIC critical period closes. Scale bar in (a) = 20μm.

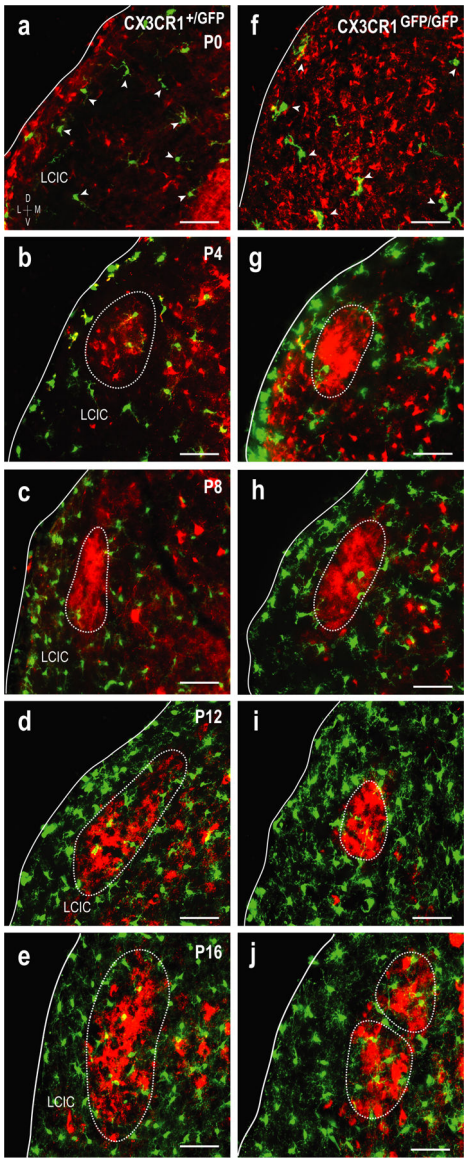

Figure 5.

Delayed MGC entry into LCIC modules in CX3CR1$^{GFP/GFP}$ mice. Comparison of the developmental progression (a-j) of MGC patterning between CX3CR1$^{+/GFP}$ (a-e) and CX3CR1$^{GFP/GFP}$ (f-j) mice. MGCs (green) with respect to emerging GAD-positive modules (red, dashed contours) at P0 (a, f), P4 (b, g), P8 (c, h), P12 (d, i), and P16 (e, j). CX3CR1-positive microglia are present at birth (arrowheads in a, f), with overall density appearing to increase with age. MGCs are largely restricted to the surrounding matrix and modular borders at P4 and P8 for both genotypes. By P12, MGCs have invaded modular confines in CX3CR1$^{+/GFP}$ but not CX3CR1$^{GFP/GFP}$ mice. This delay is transient, as MGCs occupy LCIC modules and are homogenously distributed throughout the LCIC at P16 for both genotypes. Scale bars = 50μm.

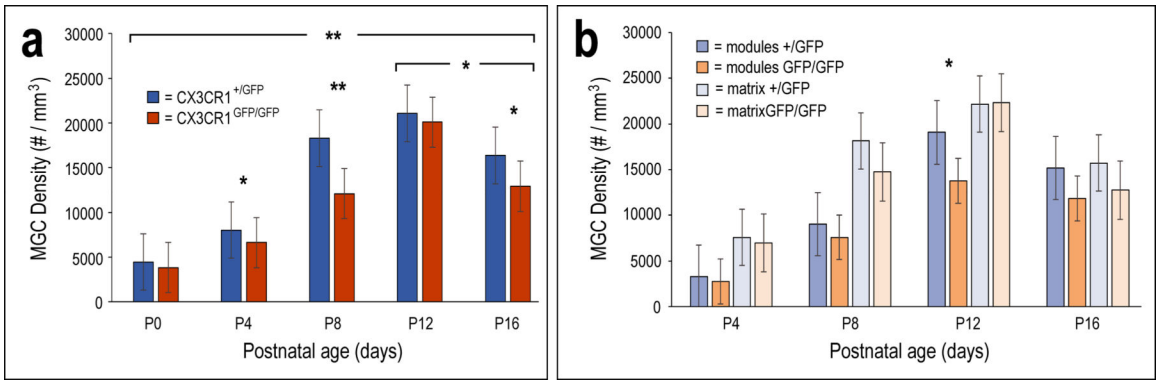

Figure 6.

Quantification of MGC density in the LCIC by postnatal age/genotype (a) as well as cell location (modular vs. matrix, b). MGC density significantly increases in the LCIC up to P12 (hearing onset), before significantly dropping by P16 in both $CX3CR1^{+/GFP}$ and $CX3CR1^{GFP/GFP}$ mice. With compromised fractalkine signaling, significantly fewer MGCs are present in the LCIC at P4, P8, and P16 compared to $CX3CR1^{+/GFP}$ littermates (a; * = $p < 0.01$, ** = $p < 0.001$). Fractalkine-mediated MGC recruitment from the surrounding matrix into modular zones is delayed in $CX3CR1^{GFP/GFP}$ mice, as significantly less MGCs occupy LCIC modules at P12 (b; * = $p < 0.05$). Restricted migration is short-lived, however, as MGC density within modules is comparable to that of heterozygous littermates by P16. P0 was not assessed for relative MGC location (modular vs. matrix) in (b) as modules do not become evident until P4. A total of n = 30 mice were included in the quantitative measures. Multiple animals were used at each age (n = 3) for each of the two genotypes (i.e. n = 6 total mice at each age). For each mouse at least 3 sections were sampled to include anatomical variability at different caudorostral levels of the LCIC. Thus, a minimum of 9 sections from a minimum of 3 animals were included for each analytical category. Error bars depict standard deviations.

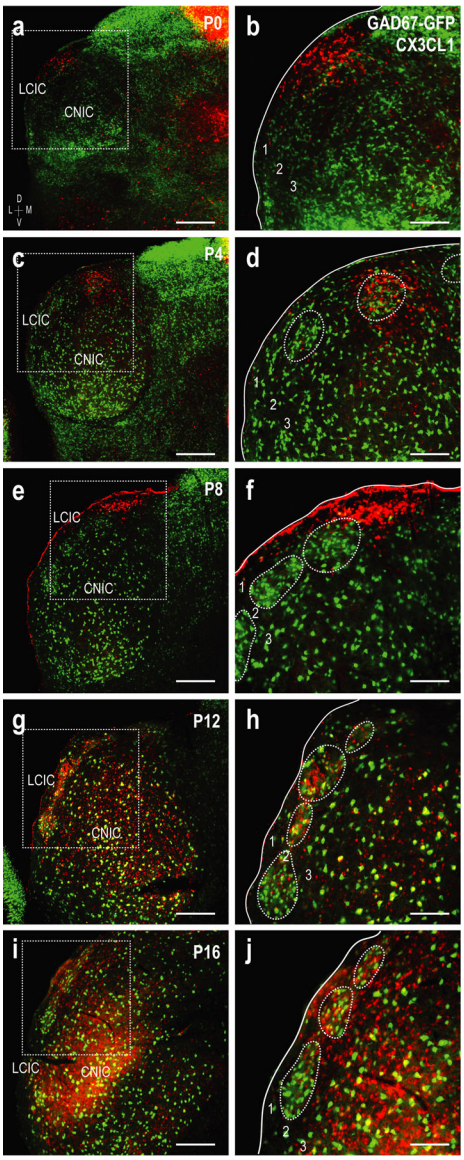

Figure 7.

Developmental progression of fractalkine (CX3CL1) expression (red) with respect to emerging GAD-positive LCIC modules (green, dashed contours) at P0 (a, b), P4 (c, d), P8 (e, f), P12 (g, h), and P16 (i, j). Inset boxes in low magnification images (a, c, e, g, i) are shown at higher magnification in (b, d, f, h, j). Sparse CX3CL1 expression at the earlier timepoints (P0-P8) exhibits a peculiar dorsal bias, prior to becoming distinctly modular at P12. Fractalkine expression is more homogeneous by P16 throughout the IC. Scale bars in (a, c, e, g, i) = 200μm; in (b, d, f, h, j) = 100μm.

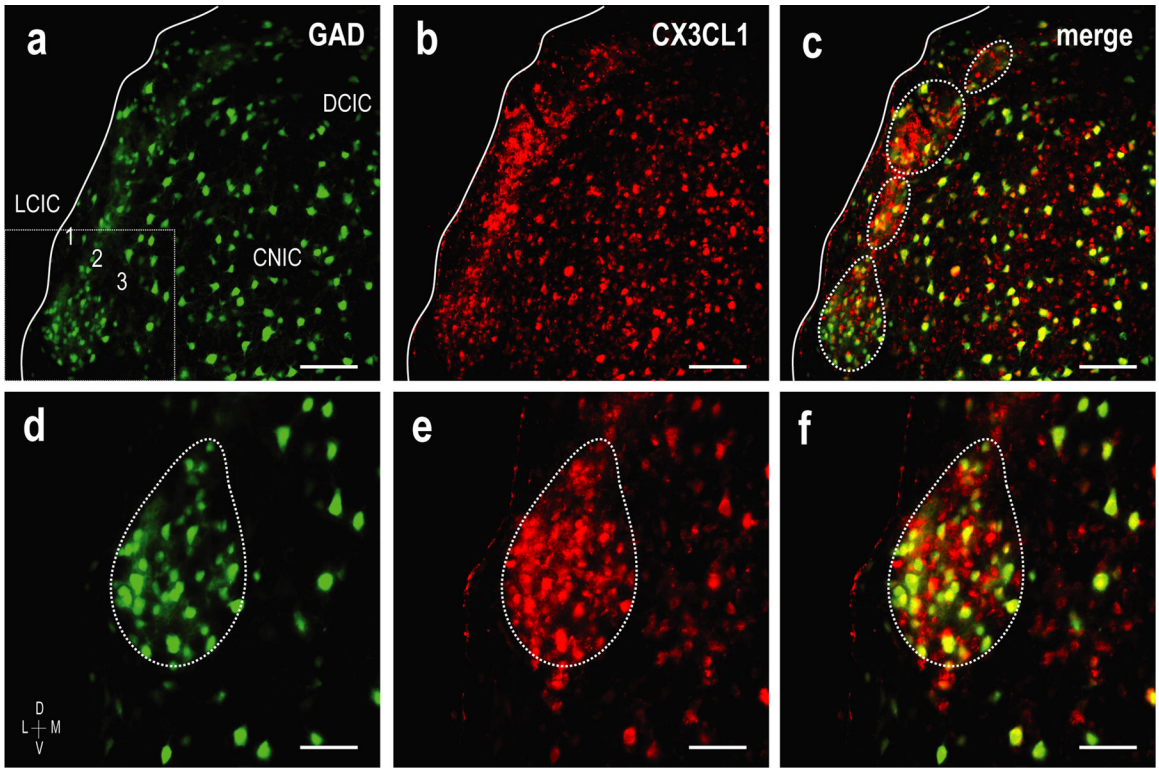

Figure 8.

Spatial overlap of GAD-defined modules (green) and CX3CL1 expression (red) at P12. In keeping with MGC recruitment into modular zones at this age as observed in CX3CR1$^{+/GFP}$ mice with functional fractalkine receptors, earlier unremarkable expression of fractalkine becomes distinctly modular at P12 (a-c). Higher magnifications (d-f) of inset box (a) show clear overlap of fractalkine expression and GAD-positive LCIC modules. While spatially aligned (i.e. modular), CX3CL1- and GAD-positive neuronal populations appear largely distinct, with few double-labeled cells (f). Scale bars (a-c) = 100μm and (d-f) = 50μm.

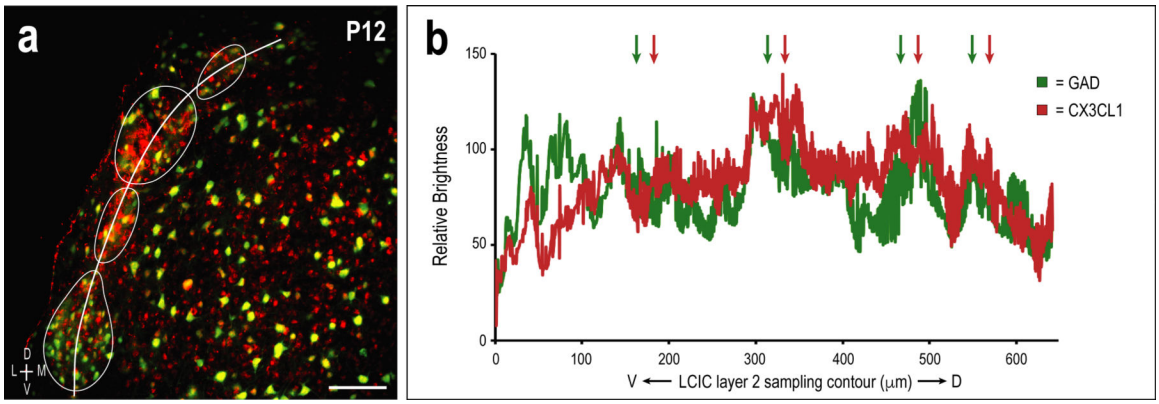

Figure 9.

Multi-channel ROI contour sampling (LCIC layer 2 modular fields) at P12 (a) with corresponding brightness plot profile showing representative overlapping signal fluctuations and relative maxima (arrows in b; correlate with aligned GAD- and CX3CL1-modular labeling). Scale bar = 100μm.

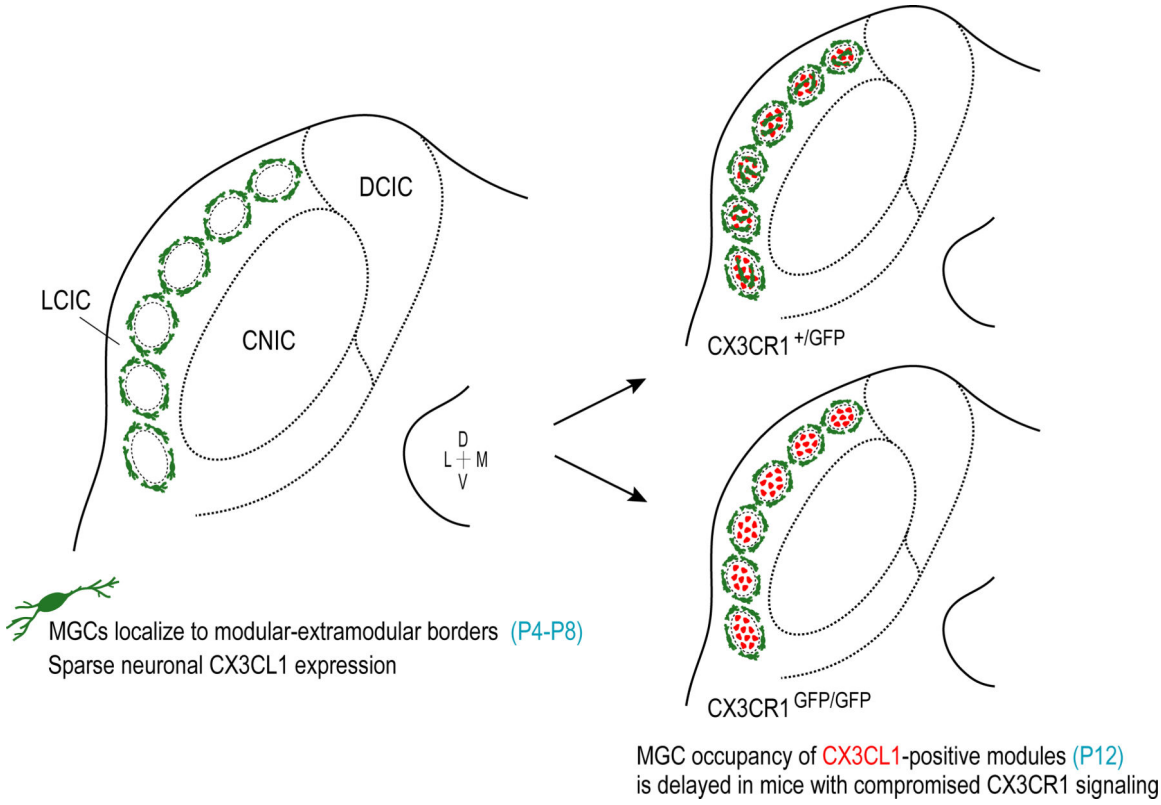

Figure 10.

Summary schematic of CX3CR1-expressing MGCs (green) and fractalkine (CX3CL1) patterns (red) over the LCIC critical period in CX3CR1$^{+/GFP}$ and CX3CR1$^{GFP/GFP}$ mice. Regardless of genotype, MGCs are present in the LCIC at birth, and surround emerging modular zones from P4 to P8. At these earliest timepoints, CX3CL1 expression is unremarkable. At P12, CX3CL1 expression becomes distinctly modular, overlapping GAD-defined zones. This upregulation correlates with MGC invasion of modular cores in mice with functional fractalkine receptors. In mice with compromised fractalkine signaling, however, MGC entry into LCIC modules at P12 is delayed. This discrepancy is albeit brief, as homogeneous LCIC microglial distributions are observed by P16 for both CX3CR1$^{+/GFP}$ and CX3CR1$^{GFP/GFP}$ mice.

Table 1.

Antibody information

Antibody name	Structure of immunogen	Manufacturer info.	Concentration used
Anti-CX3CL1/Fractalkine	*E. coli*-derived recombinant mouse CX3CL1/ Fractalkine Leu22-Lys105	R&D Systems, AF472, goat, polyclonal, RRID: AB_2276839	1:100
Anti-GAD67	Clone 1G10.2, recombinant GAD67 protein, reacts with the 67 kDa isoform	MilliporeSigma, MAB5406, mouse, monoclonal, RRID: AB_2278725	1:100
Anti-Iba1	Synthetic peptide that corresponds to the C-terminus of Iba1	Wako Chemicals, 019-19741, rabbit, polyclonal, RRID: AB_839504	1:1000
Biotinylated horse anti-goat IgG	IgG recognizes both heavy and light chains from goat	Vector Laboratories, BA-9500, horse	1:600
Biotinylated horse anti-rabbit IgG	IgG recognizes both heavy and light chains from rabbit	Vector Laboratories, BA-1100, horse	1:600
Biotinylated mouse on mouse (M.O.M.) anti-mouse IgG	IgG designed specifically to localize mouse primary antibodies on mouse tissue	Vector Laboratories, BMK-2202, mouse, RRID: AB_2336833	1:250